7 January 1997
Electronics Letters Online No: 19970299

K. Mori, H. Takara and M. Saruwatari (*NTT Optical Network Systems Laboratories, 1-1 Hikari-no-oka, Yokosuka, Kanagawa, 239, Japan*)

References

1 INOUE, K., HASEGAWA, T., ODA, K., and TOBA, H.: 'Multichannel frequency conversion experiment using fibre four-wave mixing', *Electron. Lett.*, 1993, **29**, pp. 1708–1710

2 MORIOKA, T., KAWANISHI, S., TAKARA, H., and SARUWATARI, M.: 'Multiple-output, 100Gbit/s all-optical demultiplexer based on multichannel four-wave mixing pumped by a linearly-chirped square pulse', *Electron. Lett.*, 1994, **30**, pp. 1959–1960

3 MORI, K., MORIOKA, T., and SARUWATARI, M.: 'Optical parametric loop mirror', *Opt. Lett.*, 1995, **20**, pp. 1424–1426

4 MORI, K., MORIOKA, T., and SARUWATARI, M.: 'Wavelength-shift-free spectral inversion with an optical parametric loop mirror', *Opt. Lett.*, 1995, **21**, pp. 110–112

5 MORI, K., UCHIYAMA, K., MORIOKA, T., and SARUWATARI, M.: 'Wavelength conversion with an optical parametric loop mirror', *Electron. Lett.*, 1996, **32**, pp. 2171–2172

660 and 760nm bands evidenced in a low-OH low-Cl fibre by Gaussian deconvolution of radiation-induced loss spectra

O. Deparis, P. Mégret, M. Decréton and M. Blondel

Indexing terms: Optical fibres, Radiation effects, Modelling

Gaussian deconvolution of the radiation induced absorption band, previously observed around 660nm, in a low OH low Cl pure silica core aluminium coated fibre, is used to show that the band is due to the superposition of two absorption bands at 660 and 760nm. These bands are endemic to the new type of silica used for the fibre fabrication.

Introduction: Recently, a new type of pure silica core fluorine-doped silica cladding optical fibre has been developed for application in the presence of ionising radiation. In addition to conventional radiation-resistant optical fibres, this fibre is considered as a promising potential candidate for applications such as fibroscopy [1] and diagnostics [2, 3] in the future international thermonuclear experimental reactor (ITER). Compared to conventional high OH pure silica core fibres fabricated from flame hydrolysis of $SiCl_4$, this new type of fibre is fabricated from KS-4V silica glass [4] and exhibits very low concentrations of both OH and chlorine impurities in the core. In a previous paper [5], we reported *in-situ* spectral measurements of the radiation-induced loss in a low OH low Cl aluminium coated fibre, exposed to gamma rays at 4.9kGy/h and 60°C at the CMF facility of SCK, Mol, Belgium. We observed a radiation induced absorption band around 660nm which suddenly appeared at the beginning of irradiation but then spontaneously disappeared for doses higher than 10–100 kGy. We also pointed out the fact that the suppression of this band was definitive. We related this band to the 660 and 760nm bands observed in the past, in low OH, low Cl fibres. Recently, these bands were again observed in KS-4V core fibres and fluorine-doped silica core fibres [2, 3]. Finally, our experiment [5] confirmed that the 600nm band related to non-bridging oxygen hole centres (NBOHC) is practically absent in this fibre because of the thermal annealing of NBOHCs during the aluminium coating application at high temperature [4]. Now, we report on the deconvolution of the previously measured radiation induced loss spectra [5] into several Gaussian bands associated to defect centres (so called colour centres). In this modelling, no attempt is made to take into account the radiation-induced UV bands or other possible bands induced below 500nm. This is because our experimental data are not taken down 400nm, and thus do not allow determination of the peaks of these bands.

Gaussian deconvolution: Our Gaussian deconvolution of radiation-induced loss spectra is based on the summation of four Gaussian functions of the photon energy (E) and a constant term (G_l) which stands for the additional optical losses due to temperature-induced microbending losses [1]. The value of this constant term ('grey loss') is taken to be equal to the measured induced loss at 1200nm (1.03eV).

$$A(E) = \sum_{i=1}^{4} A_{gi}(E) + G_l = \sum_{i=1}^{4} k_i e^{-\left(\frac{E-E_{ci}}{\sigma_i/2}\right)^2} + G_l$$

The only parameters of the model are the intensities (k_i) of the four Gaussian bands, which are dependent on the absorbed dose. The peak energies of the bands (E_{ci}) and their $1/e$ bandwidths (σ_i) are fixed. The first and second bands are the previously reported 660 and 760nm bands [6] which are endemic to this type of extremely pure silica [2, 3]. The peak energies of these bands are equal to 1.88 eV (660 nm) and 1.63eV (760nm) and their bandwiths are equal to 0.479 and 0.607eV, respectively (values taken from [6]). The third band, peaking at 2.40eV (516nm) with a 0.600eV bandwidth [3], would be due to an unidentified diamagnetic defect centre. The fourth band, peaking at 2.07eV (600nm) with a 0.380eV bandwidth [3], has been added to take into account the residual NBOHCs. Therefore it can be expected that the intensity of this fourth band should be weak.

Results and discussion: The results of the modelling of radiation-induced loss spectra from 500nm (2.48eV) to 1200nm (1.03eV) are shown in Figs. 1 – 3 at three different doses (from first irradiation data [5]). Because we did not model the UV bands, the strength of the 516nm band is probably overestimated, especially at high doses. At low doses (Fig. 1), the observed radiation-induced band at around 660nm stands out from the spectra because the UV band tails (and other possible bands below 500nm) are still weak

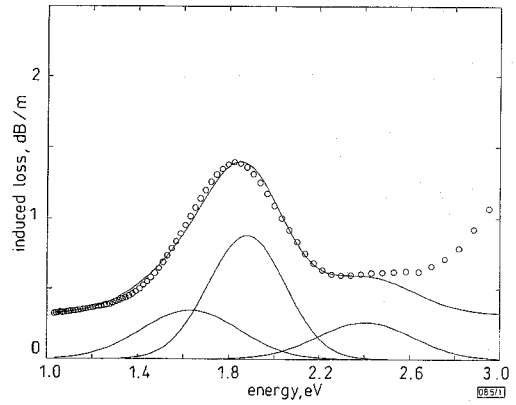

Fig. 1 *Radiation-induced loss spectra at 1.6kGy modelled by three Gaussian bands*

○ data from [5]
——— simulations - see text

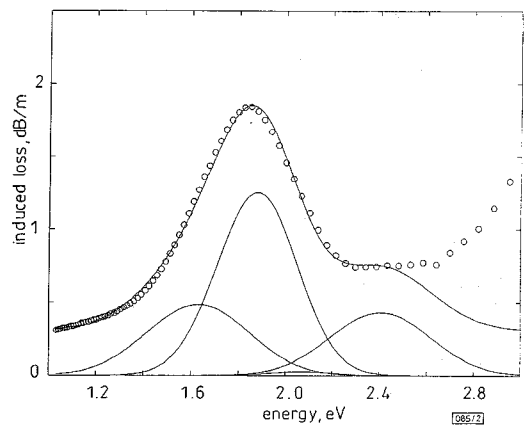

Fig. 2 *Radiation-induced loss spectra at 5.3kGy modelled by four Gaussian bands*

○ data from [5]
——— simulations - see text

[5]. In this case, only three bands (660, 760 and 516nm) are needed to correctly fit the data. The Gaussian deconvolution shows that the band we observed around 660nm is in fact due to the superposition of the previously reported 660 and 760nm bands. At higher doses (Figs. 2 and 3), the measured spectra show a diminution of the observed 660nm band with dose [5] while the overall loss increased dramatically below 500nm (above 2.48eV). A weak 600nm band is now needed to correctly fit the data. The weak intensity of this NBOHC-related band means that the concentration of these defect centres is relatively low in this type of fibre. This is consistent with the supposed thermal annealing of NBOHCs during the aluminium coating application at high temperature [4].

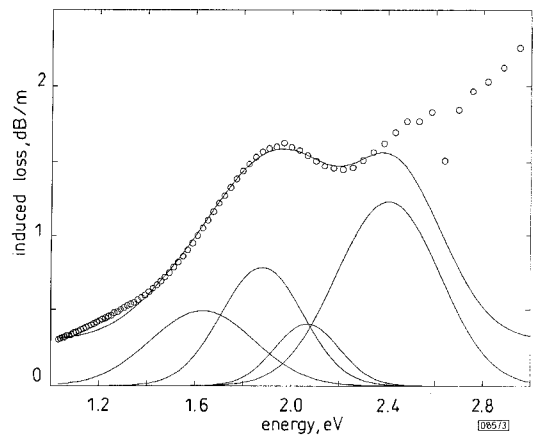

Fig. 3 *Radiation-induced loss spectra at 53.2kGy modelled by four Gaussian bands*

O data from [5]
——— simulations - see text

Conclusion: The radiation-induced loss spectra measured *in situ* during a γ-irradiation at 4.9kGy/h and 60°C in a low OH low Cl pure silica core aluminium coated fibre have been described as the summation of four Gaussian bands and a constant term which stands for temperature-induced microbending loss ('grey loss'). This Gaussian deconvolution of the spectra adds to the physical understanding of the radiation response of this new type of fibre. The existence of the 760 nm band, together with the 660nm band, has been demonstrated while it was difficult to infer the former from the measured spectra around 660nm. Moreover, the weak intensity of the 600nm band computed for this type of fibre confirms that the related NBOHC defect centres have been annealed by the application of the aluminium coating during the fabrication process. Further research is needed to investigate the physical origin of the 660 and 760nm bands which are thought to be endemic to this extremely pure low OH, low Cl silica.

28 January 1997
Electronics Letters Online No: 19970315

O. Deparis and M. Decréton and (*SCK/CEN Nuclear Research Centre, 200 Boeretang, 2400 Mol, Belgium*)

P. Mégret and M. Blondel (*Faculté Polytecnique de Mons, 31 bd Dolez, 7000 Mons, Belgium*)

O. Deparis: also with Faculté Polytecnique de Mons, 31 bd Dolez, 7000 Mons, Belgium

References

1 DEPARIS, O., MÉGRET, P., DECRÉTON, M., and BLONDEL, M.: 'Gamma radiation tests of potential optical fibre candidates for fibroscopy', *IEEE Trans. Nucl. Sci.*, 1996, **43**, (6), pp. 3027–3031

2 GRISCOM, D.L., GOLANT, K.M., TOMASHUK, A.L., PAVLOV, D.V., and TARABRIN, Y.A.: 'γ-radiation resistance of aluminium-coated all-silica optical fibers fabricated using different types of silica in the core', *Appl. Phys. Lett.*, 1996, **69**, (3), pp. 322–324

3 GRISCOM, D.L.: 'γ and fission reactor radiation effects on the visible-range transparency of aluminum-jacketed, all-silica optical fibers', *J. Appl. Phys.*, 1996, **80**, (4), pp. 2142–2155

4 BOGATYRJOV, V.A., CHEREMISIN, I.I., DIANOV, E.M., GOLANT, K.M., and TOMASHUK, A.L.: 'Super high strength metal coated low hydroxyl low chlorine all silica optical fibres', *IEEE Trans. Nucl. Sci.*, 1996, **43**, (3), pp. 1057–1060

5 DEPARIS, O., MÉGRET, P., DECRÉTON, M., and BLONDEL, M.: 'Evolution of the 660 nm radiation induced band in a low OH low Cl optical fibre', *Electron. Lett.*, 1996, **32**, (15), pp. 1392–1393

6 NAGASAWA, K., TANABE, M., and YAHAGI, K.: 'Gamma-ray-induced absorption band in pure-silica-core fibers', *Jpn. J. Appl. Phys.*, 1984, **23**, (12), pp. 1608–1613

Gain optimisation of an erbium doped fibre for remote pumping system

H. Kawakami, A. Sano and K. Hagimoto

Indexing terms: Erbium-doped fibre amplifiers, Optical pumping, Optimisation

The authors investigate the optimum length of erbium doped fibre (EDF) for a remote pumping system. The optimum EDF gain yielding the minimum total noise figure (NF) is calculated and experimental data support the theoretical analysis.

Introduction: As the need for longer unrepeated transmission distances increases, advanced transmission schemes that reduce transmission fibre loss are required. The remote pumping system based on erbium doped fibres (EDF) is an attractive scheme [1]. In a remote pumping system, the total gain and total noise figure (NF) are determined by the length of the EDF and its position in the transmission line. Maximum total gain and minimum total NF cannot be achieved simultaneously. Indeed, the quantum limit of NF defined by the population inversion factor [2], only applies to the case of high amplifier gains. The noise figure of a low gain optical amplifier, can be less than twice the population inversion factor [3]. We note that the lower limit of the EDF gain is decided by the shot noise of the transmitted optical signal [4]. The optimum EDF gain for remote pumping systems has not yet been investigated.

This Letter investigates the total NF of a remote pumping system when the distance between the pump light source and the EDF is given. We calculate the total NF against EDF gain. Our experimental data support the theoretical analysis.

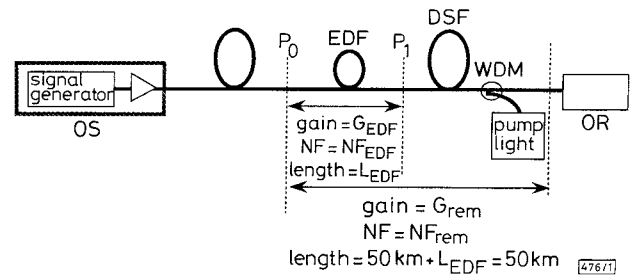

Fig. 1 *Experimental setup*

Experimental setup: Fig. 1 shows the experimental setup. The signal and pump light wavelengths were 1.55 and 1.48μm, respectively. The pump light counter-propagated through the 50km dispersion shift fibre (for 1.55μm), and launched into the EDF. The signal power level at *P*0 was –25dBm. The definitions of the parameters (NF_{EDF}, NF_{rem}, *et al.*) are also given. In this Letter, NF does not include the photodetector shot noise.

For the EDF, $\rho\sigma(1.55\mu m) = 0.269$, $\rho\sigma(1.48\mu m) = 0.188$, $Ahv/\sigma/\tau(1.55\mu m) = 0.325mW$, $Ahv/\sigma/\tau(1.48\mu m) = 0.490mW$, where ρ is the Er ion density, σ is the absorption cross-section, τ is the photon life time, *h* is Planck's constant, and *A* is the effective core area. We can calculate G_{EDF} and NF_{EDF}, using the rate equation with these parameters [5, 6].

Measured EDF characteristics are shown in Figs. 2 and 3. In Fig. 2, G_{EDF} and NF_{EDF} are shown against pump power (circles and triangles). In Fig. 3, G_{EDF} and NF_{EDF} are shown against L_{EDF} (circles and triangles). Theoretical curves are also shown in Figs. 2 and 3. The emission from the pump level must be considered in the 1.48μm pumping scheme, though it can be ignored in an ideal